

ORIGINAL RESEARCH REPORT

Full-thickness tissue engineered oral mucosa for genitourinary reconstruction: A comparison of different collagen-based biodegradable membranes

Roxana Schwab^{1,2} | Martin Heller^{1,2} | Céline Pfeifer^{2,3} | Ronald E. Unger^{2,4} |
 Stefan Walenta⁵ | Sandra Nezi-Cahn^{1,2} | Bilal Al-Nawas^{2,6} |
 Annette Hasenburger^{1,2} | Walburgis Brenner^{1,2,3}

¹Department of Gynecology, University Medical Center of the Johannes Gutenberg University Mainz, Mainz, Germany

²For BiomaTICS—Biomaterials, Tissue and Cells in Science, University Medical Center of the Johannes Gutenberg University Mainz, Mainz, Germany

³Department of Urology, University Medical Center of the Johannes Gutenberg University Mainz, Mainz, Germany

⁴Department of Pathology, University Medical Center of the Johannes Gutenberg University Mainz, Mainz, Germany

⁵Institute of Pathophysiology, University Medical Center of the Johannes Gutenberg University Mainz, Mainz, Germany

⁶Department of Maxillofacial Surgery, University Medical Center of the Johannes Gutenberg University Mainz, Mainz, Germany

Correspondence

Walburgis Brenner, Department of Gynecology, University Medical Center of the Johannes Gutenberg University Mainz, Langenbeckstr. 1, 55131 Mainz, Germany.
 Email: brenner@uni-mainz.de

Abstract

Tissue engineering is a method of growing importance regarding clinical application in the genitourinary region. One of the key factors in successful development of an artificially tissue engineered mucosa equivalent (TEOM) is the optimal choice of the scaffold. Collagen scaffolds are regarded as gold standard in dermal tissue reconstruction. Four distinct collagen scaffolds were evaluated for the ability to support the development of an organotypical tissue architecture. TEOMs were established by seeding cocultures of primary oral epithelial cells and fibroblasts on four distinct collagen membranes. Cell viability was assessed by MTT-assay. The 3D architecture and functionality of the tissue engineered oral mucosa equivalents were evaluated by confocal laser-scanning microscopy and immunostaining. Cell viability was reduced on the TissuFoil E[®] membrane. A multi-stratified epithelial layer was established on all four materials, however the TEOMs on the Bio-Gide[®] scaffold showed the best fibroblast differentiation, secretion of tenascin and fibroblast migration into the membrane. The TEOMs generated on Bio-Gide[®] scaffold exhibited the optimal cellular organization into a cellular 3D network. Thus, the Bio-Gide[®] scaffold is a suitable matrix for engineering of mucosa substitutes in vitro.

KEYWORDS

biodegradable scaffolds, coculture, primary oral epithelial cells, primary oral fibroblasts, tissue engineered mucosa equivalents

1 | INTRODUCTION

Tissue engineering is a relatively new emerging technology in the field of regenerative medicine. It developed because of the growing needs of

plastic and reconstructive surgery to restore form and function in a subset of patients with tissue damage due to preexisting or neoplastic disease, trauma or congenital anomalies on one hand, and from the need to improve aesthetic appearance after surgeries on the other.¹ Thus, it is not surprising that skin was one of the first engineered tissues to be used in the clinical setting.¹ Humby first described the successful use of buccal mucosa for reconstruction surgery in males with hypospadias in

[Correction added on 18 September 2020, after first online publication: Projekt Deal funding statement has been added.]

This is an open access article under the terms of the Creative Commons Attribution License, which permits use, distribution and reproduction in any medium, provided the original work is properly cited.

© 2020 The Authors. *Journal of Biomedical Materials Research Part B: Applied Biomaterials* published by Wiley Periodicals LLC.

1941.² In the following decades, several other targets of reconstructive surgery in the maxillofacial region were described, for example, in correcting defects in the conjunctiva, larynx, and trachea.^{3,4}

Skin and mucosal defects involving the genitourinary region arise from acquired or innate conditions. Congenital malformations such as cloacal malformation and vaginal aplasia in females or hypospadias in males, as well as acquired disorders such as cancer or trauma often lead to extended damage and loss of skin tissue located in the genitourinary area.⁵⁻⁹ For these purposes, reconstructive surgery evolves to a challenging procedure because of lack of available and appropriate tissue.⁵⁻⁹ Recently, tissue engineered mucosa equivalents with autologous cells for reconstruction of genitourinary structures have been reported and were used in a number of different applications.^{7,8,10-12}

The main goal of both tissue engineering and reconstructive surgery is to restore form and function in combination with minimal morbidity.^{12,13} One crucial benefit of tissue engineering compared to established reconstructive surgery procedures, such as skin grafts or (myo-)cutaneous flaps, is minimizing the degree of surgical intervention. The best results for obtaining optimal aesthetic and functional characteristics were described after repairing the defects using a similar tissue.¹⁴

Buccal grafts have been successfully used for urethral^{12,15} and vaginal reconstruction with autologous tissue,¹⁴ since both anatomical regions are covered by a nonkeratinized epithelium of endoderm origin.¹⁶ Short-term and long-term donor site morbidity following large buccal biopsies, such as oral pain and numbness, as well as possible reduced mouth opening and altered salivation, restricted the amount of harvested tissue^{12,17,18} and encouraged the concept of tissue engineered products with in vitro expanded autologous cells derived from small buccal biopsies.^{12,19} Considering the small amount of buccal mucosa tissue needed to extract primary epithelial cells and fibroblasts, and due to the possibility of growing and expanding these cells in vitro to obtain an adequate number of cells for covering the required area of a wound, tissue engineered buccal mucosa proved as a valuable construct for reconstruction purposes in the genitourinary area.

Skin or mucosal generation using tissue-engineering methods resembles skin regeneration during wound healing. In both cases, the availability of vital and appropriate cell types, their potential to proliferate, migrate and to generate an adequate extracellular matrix in a highly complex and orchestrated manner, as well as the need of an optimal microenvironment, is crucial for the development of a 3D network of cells reassembling the desired tissue.^{13,20} During natural wound healing, a fibrin clot is initially formed and acts as a matrix directing the cellular proliferation, migration, and reorganization of the tissue. In tissue engineering, the choice of the scaffold is crucial for the success of the formation of the desired 3D tissue construct.^{13,20} Optimal scaffolds support cell adherence, proliferation, differentiation and migration, allowing the development of a 3D engineered tissue. Scaffolds are normally used in vitro as substitutes for the extracellular matrix molecules required during the physiological wound healing process, helping to form the structure of the engineered tissue. The scaffold must meet certain prerequisites prior to clinical implementation, such as membrane stability and maintenance of the optimal environment for tissue regeneration.^{13,21} Collagen-based biomaterials, such as Bio-Gide® (BG), Bio-

Gide-Pro® (BGP), TissueFoil E® (TF), or Surgisis® ES (SIS) are the gold standard for wound healing purposes. They are biodegradable and biocompatible and, due to the highly conserved interspecies collagen structure, no immunological rejection is expected.^{13,21,22}

The aim of the study was to determine the appropriate collagen scaffold in terms of in vitro cellular growth, migration, differentiation, and formation of a full-thickness tissue engineered oral mucosa equivalent for reconstruction purposes in the genitourinary region.

2 | MATERIALS AND METHODS

2.1 | Cell isolation and culture of primary cells in mono-layers

Samples of normal human oral mucosa were obtained from superfluous buccal tissue, and were used to isolate primary epithelial cells and fibroblasts. The Ethics Committee of *Landesärztekammer Rheinland-Pfalz* (No. 837.439.05 (5097)) approved the study regarding tissue engineered oral mucosa with autologous cells. This study included only clinically healthy donors undergoing dental procedures after informed consent.

For cultivation of primary epithelial cells, the mucosal biopsy was incubated briefly in 70% ethanol for surface disinfection and then rinsed with phosphate buffered saline. The epithelium was mechanically separated from the lamina propria and digested with dispase II (240 U/100 ml; Roche, Mannheim, Germany) for 30 min at 37°C. Afterward, the tissue was cut into pieces of approx. 4 mm² and placed into a T-25 flask (Greiner, Frickenhausen, Germany). Primary epithelial cells grew out from the adherent tissue pieces after being cultured in FAD-complete-medium: DMEM (Sigma-Aldrich, Steinheim, Germany) supplemented with 30% DMEM/Ham's-F12 (BiochromAG, Berlin, Germany), 10% fetal calf serum (FCS) (PAA, Pasching, Austria), 90 U/ml penicillin G sodium, 90 U/ml streptomycin sulfate, 0.225 µg/ml amphotericin B (Gibco, Life Technologies GmbH, Eggenstein, Germany), 22 µg/ml adenine, 7.4 ng/ml cholera toxin, 9 ng/ml EGF, 36 ng/ml hydrocortisone, and 4.6 µg/ml insulin (Sigma-Aldrich, Steinheim, Germany). Cells were incubated at 37°C with 5% CO₂ and medium was changed every 2-3 days.

To cultivate primary oral fibroblasts, mucosal connective tissue was cut into 1 mm² cubes. The pieces were placed into T-75 flasks and cultured with DMEM supplemented with 10% FCS, 90 U/ml penicillin G sodium, 90 U/ml streptomycin sulfate, and 0.225 µg/ml amphotericin B until cells grew out of the pieces. The subconfluent cells were detached with 0.25% trypsin/0.02% EDTA-solution (Sigma-Aldrich, Steinheim, Germany) and passaged. The primary epithelial cells and fibroblasts were expanded for a minimum of 10 days before splitting and used approximately 20 days after isolation in the third or fourth passage.

2.2 | Membranes examined

Three commercially available (Bio-Gide®, TissuFoil E®, Surgisis® ES) and one non-commercially available (Bio-Gide-Pro®) biodegradable

membranes were tested for generation of a 3-dimensional mucosa tissue (Table 1):

1. Bio-Gide® (Geistlich Biomaterials, Wolhusen, Switzerland): porcine skin-derived bi-layered membrane of non-cross-linked types I and III collagen.²³
2. Bio-Gide-Pro® (Geistlich Biomaterials, Wolhusen, Switzerland): porcine skin-derived bi-layered membrane of 1-ethyl-3-(3-dimethylaminopropyl)-carbodiimide (EDC)/N-hydroxysuccinimide (NHS)-cross-linked porcine types I and III collagen.²³
3. TissuFoil E® (Baxter Immuno Inc., Heidelberg, Germany): non-cross-linked equine type I collagen with a density of 4 mg collagen/cm², thickness 1 mm.²⁴
4. Surgisis® ES (Cook Biotech Inc., West Lafayette, IN): porcine-derived collagen-based small intestinal submucosa (non-cross-linked collagen I, III, V) with extracellular matrix components (glycosaminoglycans, proteoglycans, growth factors).²⁵⁻²⁷

2.3 | Seeding of fibroblasts on the membranes

The membranes were stamped with punches to obtain circular discs measuring 6 mm in diameter. Before seeding, membranes were rehydrated in sterile phosphate buffered saline, according to the manufacturers' instructions (SIS and BGP overnight, BG and TF: 10 min at 20°C). Fibroblasts were trypsinized using 0.25% trypsin/0.02% EDTA, and 2×10^5 cells/cm² were seeded in a 24-well plate onto the mono-layer matrices TF and SIS and on the cell-non-occlusive side of the bi-layered membranes BG and BGP. The membranes with cells were incubated for 4 hr at 37°C to allow for the attachment of the cells to the respective membranes. Afterward, the membranes were transferred to a culture dish, and the seeded fibroblasts were cultivated in DMEM supplemented with 10% FCS, 90 U/ml penicillin G sodium, 90 U/ml streptomycin sulfate and 0.225 µg/ml amphotericin B. The medium in the dishes was replaced every 48 hr.

2.4 | Cell viability

The viability of the cells seeded on cell culture plastic as control group was compared to cells seeded on the distinct membranes, and was examined in 48-well plates using the MTT 3-(4,5-dimethylthiazol-2-yl)-2,5-diphenyltetrazolium bromide) assay (Sigma-Aldrich Chemie GmbH, Taufkirchen, Germany) after 3, 5, 14 days of cell culture. Unseeded bio-membranes punches were used as negative controls. After 3, 5, or 14 days, supernatant from each well was replaced with an equal volume of MTT solution accordingly to the manufacturer's instructions. After incubation for 2 hr at 37°C, the supernatant was removed and discarded and the blue formazan reaction product remaining in the wells was dissolved by adding equal volume of solubilization solution. After 3 hr on a platform shaker at 500 rpm, 100 µl supernatant was transferred to a 96-well plate, and the absorbance was measured at 570 nm using an Anthos 2010 spectrophotometric microplate reader (Anthos Labtec Instruments, Cambridge, GB). Cell vitality was measured as extinction in an MTT assay and showed as percentage of equal amount of cells growing on cell culture plastic as control. The assays were performed in triplicate for each time point and for each membrane.

2.5 | Measurement of diameter changes of the various bio-membrane punches

To determine the influence of cells on the structures of the various materials, fibroblasts were inoculated onto the membrane punches as described above. On day 7, cocultures with primary human oral epithelial cells (2×10^5 cells/cm²) were established in culture wells of 15 mm in diameter. During the cultivation period (days 0, 3, 7, 10, 14), the diameters of the bio-membrane punches of the various membranes were measured twice for each sample at an orthogonal angle using a caliper gauge. The changes of the diameters were indicated as percentage of the original diameter and calculated as the average of three independent experiments.

TABLE 1 Characteristics of the collagen scaffolds used in this study²³⁻²⁷

Scaffold	Bio-Gide®	Bio-Gide-Pro®	TissuFoil E®	Surgisis® ES
Corporation	Geistlich Biomaterials, Wolhusen, Switzerland	Geistlich Biomaterials, Wolhusen, Switzerland	Baxter Immuno Inc., Heidelberg, Germany	Cook Biotech Inc., West Lafayette, IN
Origine	Xenogenic (porcine skin)	Xenogenic (porcine skin)	Xenogenic (equine)	Xenogenic (porcine small intestinal mucosa)
Collagen type	Non-cross-linked types I and III collagen	1-Ethyl-3-(3-dimethylaminopropyl)-carbodiimide (EDC)/N-hydroxysuccinimide (NHS)-cross-linked porcine types I and III collagen	Highly purified non-cross-linked type I collagen	Non-cross-linked collagen I, III, V
Layering	Bi-layered	Bi-layered	Mono-layered	Mono-layered
Thickness ^a	0.5 mm	0.5 mm	1 mm	0.05–0.22
Resorbability	Yes	Yes	Yes	Yes

^aOwn measurements.

2.6 | Culture of tissue engineered organotypic oral mucosa

To generate tissue engineered oral mucosa equivalents (TEOMs), fibroblasts were first inoculated onto membrane punches of the distinct materials as described above. After 4 days of culture, primary oral epithelial cells were seeded at the same concentration of cells onto the opposite side of the matrices in a volume of 1 ml of FAD-complete medium. The cocultures of epithelial cells and fibroblasts on the various membranes were cultured organotypically at the air-medium interface in a transwell system (Netwell, Corning Inc., Schiphol-Rijk, Netherlands) in combination with a deepwell plate (BD Falcon, Franklin Lakes, NJ). One milliliter of FAD-complete culture medium was placed under the transwell insert and changed twice a week for a total cultivation period of 20 days. Under liquid/air cultivation conditions the epithelial cells differentiated, and nutrients were delivered by diffusion from below.²⁸

2.7 | Vital microscopy

After 20 days of coculture cultivation, the various membranes were removed from the growing medium, washed with sterile PBS and stained with 1 mg/ml calcein AM (Invitrogen, Eugene, OR) in PBS at 37°C at 5% CO₂. After 10 min, free calcein AM was removed by washing several times with PBS. Stained samples were assessed with a confocal laser-scanning microscope (Leica-TC SP2, Zeiss, Jena, Germany) at an excitation wavelength of 494 nm and an emission of 540 nm (green). The images were evaluated with the Leica Confocal analyzing system, which enabled an overlapping view of 50 different images, correspondent to 160 µm membrane thickness.

2.8 | Preparation and staining of histological specimen

Tissue-engineered oral mucosa-punches were fixed in 4% phosphate-buffered formaldehyde-solution for at least 1 day and embedded in paraffin. For subsequent investigations, pretreatment of deparaffinized and rehydrated 4 µm sections was performed in a steamer for at least 1 hr.

Membranes with cells were histochemically analyzed by Masson Goldner trichrome staining. This staining combines the precise staining of hematoxylin and eosin stain with a reliable cytoplasmic staining and at the same time it provides a very selective stain for the connective tissue.²⁹ Nuclei were labeled subsequently with an iron hematoxylin stain for histological examination. With this method, collagen was stained green, cell nuclei were stained dark brown to black and cytoplasm was stained red.

Immunohistochemical analyses of cytokeratin 13, tenascin, and collagen IV were performed for visualization of the epithelial cells, the

fibroblasts (indirect evidence) and the basement membrane. Membranes with cells were incubated with mouse-anti-human cytokeratin 13 antibody (1:100), mouse-anti-human tenascin antibody (1:2000), and mouse-anti-human collagen IV antibody (1:250) (all Sigma-Aldrich, Taufkirchen, Germany) at room temperature for 1 hr. The detection of the primary antibodies was carried out using the LSAB+ System-HRP Rabbit/Mouse/Goat (DAB+)-kit (Dako, Carpinteria, CA) following the manufacturer's instructions. Mayer's hematoxylin solution was used as a counterstain in immunohistochemical analysis.

2.9 | Scanning electron microscopy (SEM)

Samples for SEM were prepared using standard procedures. Membranes were fixed using 2% glutaraldehyde and 2.5% paraformaldehyde in 0.1 M cacodylate buffer (EMD Biosciences) for 1 hr at room temperature. Afterward, they were rinsed in cacodylate buffer and dehydrated in an ethanol gradient. Further, samples were dehydrated in hexamethyldisilazane for 10 min and dried overnight, then sputter coated with gold and analyzed using a Tescan-Vega microscope with an accelerating voltage of 30 kV.

2.10 | Statistical analysis

Data are presented as mean value ± SD. Comparison between groups were conducted using 2-sided Student's *t*-test. The level of statistical significance was set at $p < .05$.

3 | RESULTS

3.1 | Evaluation of the various scaffolds

3.1.1 | Structure of the distinct membranes

The macroarchitecture of the different scaffolds was observed using SEM. Both sides of the native membranes were examined by SEM, revealing morphological differences between the membranes and between the respective upper and lower side of the membranes (Figure 1). The TF membrane showed a smooth and compact upper and lower side with no pores visible (Figure 1). The structure of the other membranes exhibited a more heterogeneous texture regarding the arrangement of the collagen fibers, as well as a higher porosity (Figure 1).

3.1.2 | Shrinkage of bio-membranes during cocultivation of primary human oral fibroblasts and epithelial cells

During cocultivation of primary epithelial cells and fibroblasts on the various membranes, the BG membrane showed a significant tendency

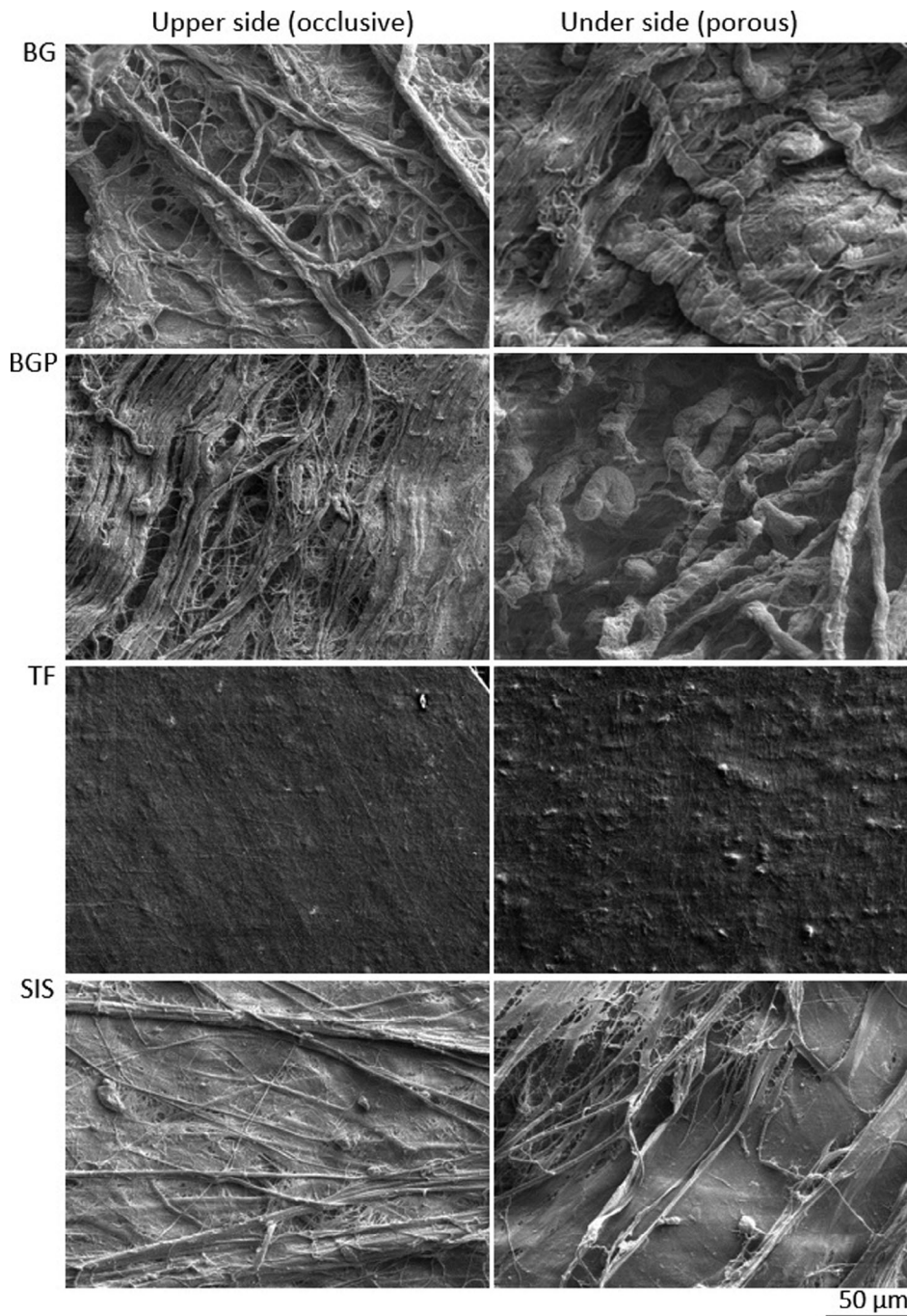


FIGURE 1 Scanning electron microscopy (SEM) photo of both sides of the various biodegradable membranes Bio-Gide® (BG); Bio-Gide-Pro® (BGP); TissuFoil E® (TF); and Surgisis® ES (SIS). On the left, SEM photo showed the occlusive, upper side of each of the four membranes. On the right, SEM photo showed the porous, lower side of each of the four membranes, respectively. Scale bars represent 50 μm

toward an alteration in shape and shrinkage in the area containing cells (Figure 2). This effect was time-dependent and was visible beginning on day 3 after seeding the primary oral fibroblasts. The shrinkages was more attenuated during the coculture with primary oral human epithelial cells, resulting in an almost 40% surface loss on day 14 (Figure 2). In contrast, the other three membranes (BGP, TF, SIS) retained their shape and their surface area during cell culture (Figure 2).

3.2 | Biocompatibility of the various matrices in vitro

3.2.1 | Effect of the various scaffolds on cellular metabolic activity

Cell viability, proliferation, and cytotoxicity are indicative of the cellular compatibility and appropriateness of the scaffolds used during the

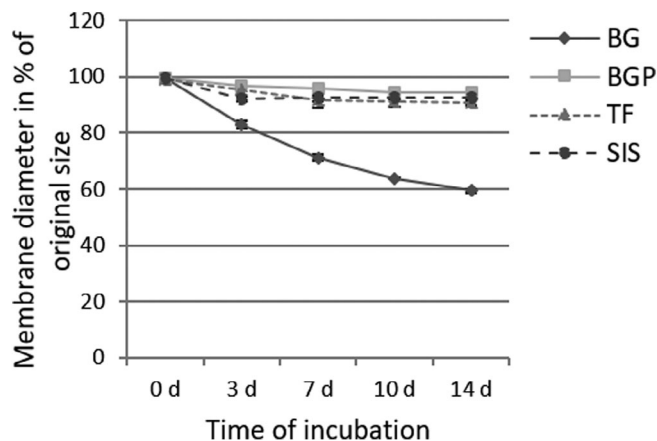


FIGURE 2 Shrinkage of bilaterally seeded bio-membranes Bio-Gide® (BG), Bio-Gide-Pro® (BGP), TissuFoil E® (TF), and Surgisis® ES (SIS). Primary human fibroblasts were seeded with a concentration of 4.15×10^4 cells/cm² on the distinct membranes (diameter 8 mm) and cultivated in culture wells (diameter 15.7 mm). On day 7, cocultures with primary human oral epithelial cells (concentration of 2×10^5 cells/cm²) were established in culture wells of 15 mm in diameter. Shrinkage of the surface of the distinct membranes during the coculture period was assessed on day 3, 7, 10, and 14. Data are shown as diameter in percent of day 0 original size. Experiments were conducted in triplicate. Shown are mean values and standard deviation. *Indicates $p < .05$ (Student's *t*-test)

tissue engineering process. In order to evaluate the cell vitality and proliferation, as well as for assessment of the cytocompatibility of the scaffolds, we performed an MTT assay after seeding equal amounts of primary fibroblasts on the various membranes. Compared to the control group (cells seeded on cell culture plastic), cells seeded on BG showed a total vitality of 120% (Figure 3). At this density, the total vitality of cells on BGP was 152% on day 3 after seeding. The cells seeded on TF and SIS reached a vitality of 93% and respective 163% on day 3 (Figure 3).

3.2.2 | Morphological characterization of the cellular layers of TEOMs engineered on the various membranes

The morphology of TEOMs was evaluated by vital staining of the cells with calcein AM and recorded in a confocal laser-scanning microscope (Figure 4). The epithelial cell layers on BG, BGP, and SIS showed a typical morphology, whereas the epithelial cell layer on TF showed a non-homogeneous arrangement of cells building both clusters and naked membrane areas, and the cells did not exhibit a typical morphology (Figure 4).

Fibroblasts seeded on BG showed a typical morphology and three-dimensional growth, whereas the cells seeded on BGP displayed an elongated cell morphology. Fibroblasts seeded on TF and SIS did not exhibit typical fibroblast morphology. Fibroblasts exhibited flat cell shapes on the TF membrane and did not form a dense cellular

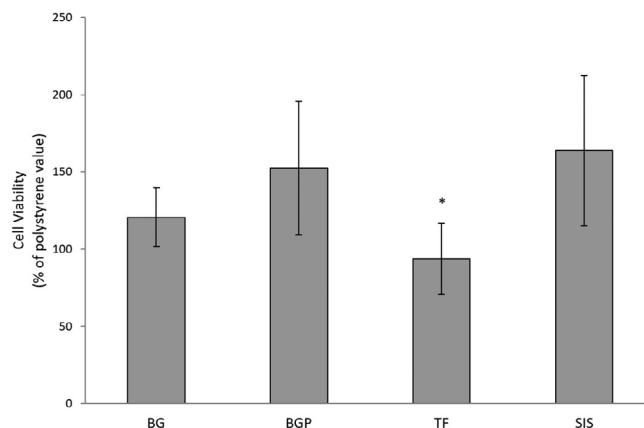


FIGURE 3 Metabolic activity of primary oral fibroblasts on various bio-membranes: Bio-Gide® (BG), Bio-Gide-Pro® (BGP), TissuFoil E® (TF), and Surgisis® ES (SIS). MTT assay was performed on day 3 after seeding 2×10^5 fibroblasts/cm² on each of the four membranes and on polystyrene surface as control group. Cell vitality was measured as extinction in an MTT assay and shown as percentage of equal amount of cells growing on cell culture plastic as control. Experiments were conducted in triplicate. Shown are mean values and standard deviation. *Indicates $p < .05$ (Student's *t*-test) referred to all other membranes

network, resulting in areas where the naked membrane was visible (Figure 4).

3.2.3 | Histology of TEOMs

Cross sections of the TEOMs were stained by Masson-Goldner for histological analysis. Each single TEOM displayed multi-layered epithelial cells on the upper side of the respective membrane, detectable by multi-layered dark-brown to black stained cellular nuclei (white arrow). On the upper side of the membranes, the cells were arranged in three to six layers (white arrow). On the lower side of the membranes, mono-layered fibroblast cells were detected in each TEOM (black arrow) (Figure 5a). Since the main component of the membranes was collagen, all four biodegradable scaffolds were stained green using the Masson-Goldner staining method. The staining of TF demonstrated the compact structure of this membrane (Figure 5a), whereas the Masson-Goldner staining of BG, BGP, and SIS revealed a more porous structure (Figure 5a). The fibroblasts were able to penetrate the porous BG membrane, but did not penetrate the BGP, TF, or SIS membranes (Figure 5a).

3.2.4 | Characterization of epithelial cells and fibroblasts in TEOMs

The distribution of epithelial cells and fibroblasts, as well as the organotypical structure of the distinct matrices, were assessed by immunohistological stainings (Figure 5b–c).

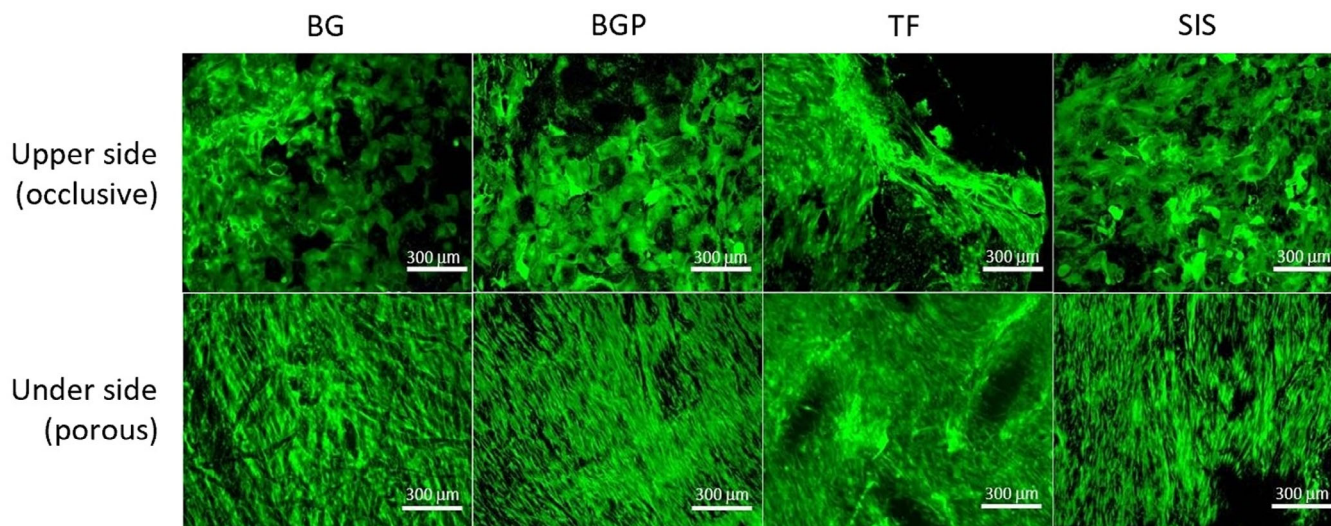


FIGURE 4 Morphology of primary human oral fibroblasts and epithelial cells in tissue engineered oral mucosa equivalents (TEOMs) using four biodegradable membranes: Bio-Gide® (BG), Bio-Gide-Pro® (BGP), TissuFoil E® (TF), and Surgisis® ES (SIS). Primary human oral fibroblasts were added to the materials at a seeding density of 2×10^5 cells/cm² and cultured for 4 days. Afterward, primary human oral epithelial cells (seeding density 2×10^5 cells/cm²) were seeded on the materials as described in Materials and Methods. On day 20, vital staining with calcein AM was carried out and membranes were examined using a confocal laserscanning microscope. Representative images of primary human oral epithelial cells on the upper side and primary human oral fibroblasts on the lower side of all four membranes are shown. The upper line represented the upper view and the bottom line the lower view of the seeded membranes. Shown are representative images. Scale bars represent 300 μ m

Epithelial cells were visualized by immunohistochemical staining of cytokeratin 13 and fibroblasts by staining of tenascin, an extracellular matrix glycoprotein secreted by fibroblasts. In all TEOMs, the cells on the upper side of the coculture expressed cytokeratin 13 as marker for epithelial cells (white arrow) (Figure 5b). No cytokeratin 13 expression was observed within the fibroblast cell layer on the lower side of the various membranes (black arrow) (Figure 5b).

A strong tenascin expression was identified within the fibroblast cell layer on the lower side of the membranes, but no tenascin was expressed within the epithelial cell layer growing on the upper side (Figure 5d). Except for the epithelial cell layer, the BG membrane was strongly stained reddish-brown for tenascin. This finding showed the growth of fibroblasts into and within the BG membrane, resulting in the formation of a three-dimensional tissue-like structure (Figure 5d). BGP showed a similar but attenuated effect (Figure 5d), whereas SIS showed a weak staining and TF showed no tenascin staining (Figure 5d).

3.2.5 | Collagen IV formation in TEOMs

In order to assess the organotypical development, cross sections of all TEOMs were immunohistochemical stained for collagen type IV, a basement membrane component. In all four types of cocultures, collagen IV was detectable basal to the epithelial cell layer, all along the interface between the epithelium and the various membranes (Figure 5c). The basement membrane formed a very thin area between the epithelial cell layer and the SIS membrane, but was thicker between the epithelial layer and the BG and the BGP membranes and

strongly pronounced between the epithelial cell layer and the TF membrane. Collagen was expressed within the fibroblast cell layers of all membranes.

4 | DISCUSSION

The aim of this study was to determine the most suitable collagen membrane in terms of structural stability and biocompatibility for the development of an organotypic tissue engineered oral mucosa equivalent. With respect to the known influence of 3D architecture of the scaffolds on the development of engineered tissue, we selected a range of collagen membranes with different collagen types and different alignment of the collagen fibers. Biocompatibility is defined as the ability to support cellular growth, differentiation, and secretion of extracellular matrix molecules, both *in vitro* and *in vivo*.³⁰ In this study, the various scaffolds were evaluated for their biocompatibility during *in vitro* conditions. Previous studies have shown that different collagen membranes could influence cellular proliferation in a specific way.^{31,32} Cells seeded on non-cross-linked collagen type I and III membranes showed increased cellular proliferation, compared to proliferation on other membranes.^{31,32} We observed no significant difference between buccal fibroblasts proliferation on the porous side of the BG membrane, compared to fibroblasts grown on cell culture plastic surfaces after 72 hr of culture. However, the source of primary fibroblast may impact the growth pattern on the porous side of the BG membrane, as human gingival fibroblasts showed a diminished growth pattern in other studies.^{31,32} To our knowledge, this is the first study to evaluate the growth pattern of fibroblasts on the BGP

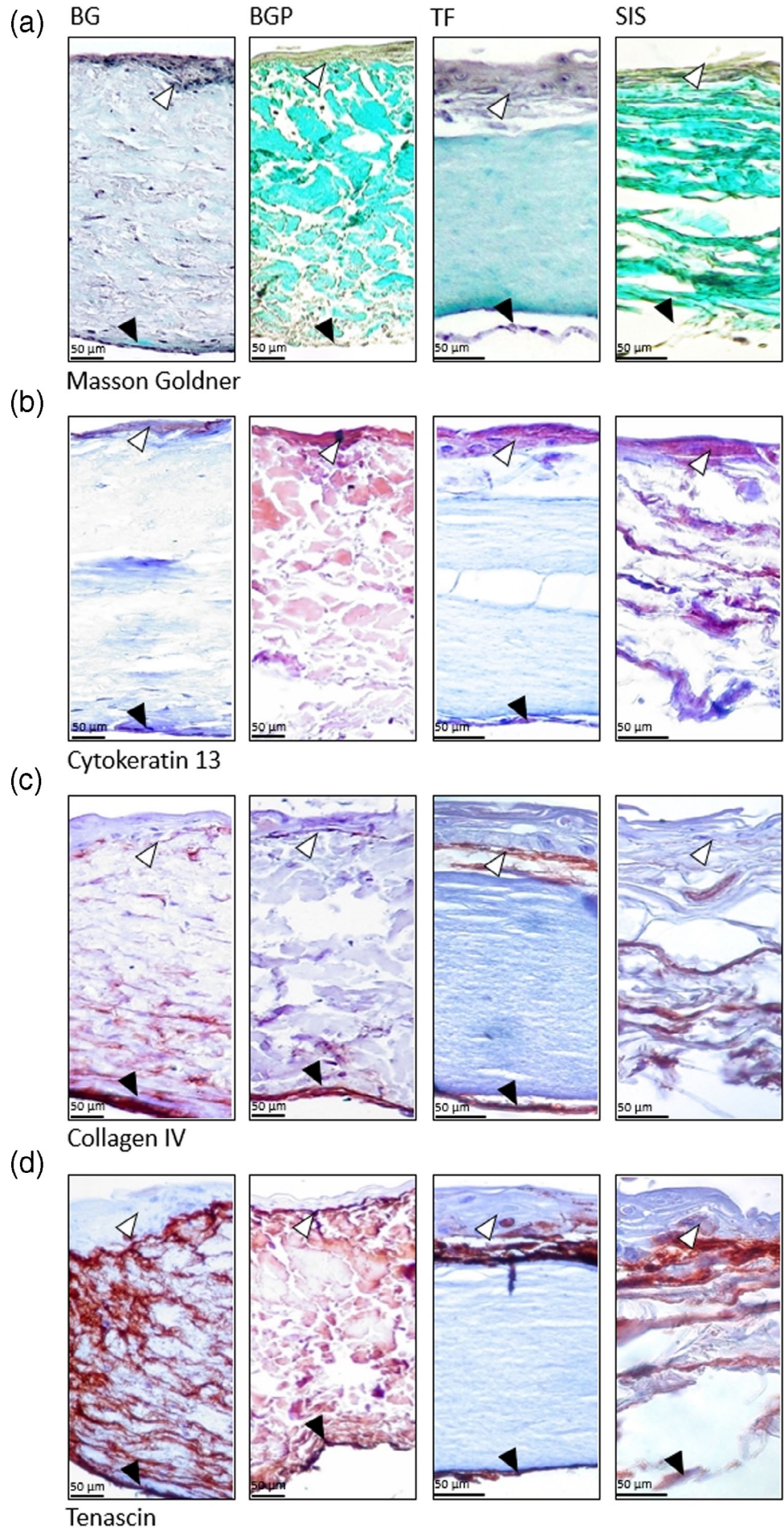
FIGURE 5 Characterization of tissue engineered oral mucosa equivalents (TEOMs).

Representative cross sections of TEOMs after 20 days of culture on the four various membranes: BioGide® (BG), BioGide-Pro® (BGP), TissuFoil E® (TF), and Surgisis® ES (SIS). Primary human oral fibroblasts were inoculated with a seeding density of 2×10^5 cells/cm² for 4 days.

Afterward, a coculture with primary human oral epithelial cells (seeding density 2×10^5 cells/cm²) was established on each of the distinct membranes. On day 20, immunohistochemical analyses were performed. Shown are representative images. Scale bars represent 50 μ m. (a) Masson-Goldner stained cross sections of TEOMs. Collagen is stained green, cell nuclei are stained dark brown to black and cytoplasm is stained red. White arrows: multi-layered epithelial cells; black arrows: mono-layered fibroblasts.

(b) Cytokeratin 13 expression as a marker for stratified epithelium in TEOMs. Cytokeratin 13 is stained reddish-brown, nuclei are stained blue. White arrows: cytokeatin expression within multi-layered epithelial cells; black arrows: no cytokeatin staining within the fibroblast cell layer. (c) Collagen IV staining as marker for basal membrane formation in TEOMs. Collagen IV is stained reddish brown. White arrows: collagen IV connecting the multi-layered epithelial cells and the distinct membranes; black arrows: collagen IV connecting the fibroblasts with the distinctive membranes.

(d) Tenascin expression in TEOMs. Tensacin is stained reddish brown. White arrows: lack of tenascin staining within the multi-layered epithelial cells; black arrows: intensive staining within the fibroblast layer



membrane. The BGP scaffold, a bi-layered crosslinked porcine type I and III collagen membrane, enhanced proliferation of buccal fibroblasts, but without statistical significance compared to the BG membrane. In contrast, the non-cross-linked equine matrix TF exhibited a significant reduction in proliferation, compared to the porcine-derived collagen membranes BG, BGP, and SIS. Nevertheless, all four membranes showed an adequate biocompatibility, since fibroblasts grew on all four scaffolds.

One of the main problems of tissue engineering is finding an optimal scaffolding material.¹³ Ideally, the selected membranes should remain stable in form during the *in vitro* culture period and degenerate with time after implantation, but without inducing foreign body reactions.¹³ In the present study, three membranes retained their original surface structure during a culture period of 14 days, whereas the BG membrane exhibited significant shrinkage within 3 days after adding cells, and finally lost 40% of its original diameter by day 14. The shrinkage effect should be considered during the *in vitro* generation of suitable TEOMs on the BG membrane. For clinical applications, the shrinkage could be compensated by choosing a larger BG membrane than the expected area at the transplantation site.

The membranes used in this study are of xenogeneic origin. Nevertheless, they are suitable for application in humans, since collagen is highly conserved across different species and, therefore, rejection is not expected.²² Additionally, collagens are the most abundant proteins in the human body and the dominant structural component of connective tissue.²¹ Therefore, collagen membranes are regarded as the gold standard for applications in wound healing despite the availability of alternative scaffolds such as acellular matrices or synthetic biodegradable polymers.²¹ Hence, membranes composed of collagen I and/or III could be an ideal scaffold for the generation of TEOMs, since the cells seeded on the respective membranes are exposed to components of the extracellular matrix similar to those in wounds. These are essential requirements to encourage cell growth and migration.³³ However, an optimal coverage of the membrane and an optimal cellular architecture was only observed in TEOMs generated on the BG membrane, but not in TEOMs generated on BGP, TF, or SIS, although all membranes examined in this study were composed of collagen I and III, with the exception of TF, which contained only collagen I. In addition, the cellular network formed on the TF membrane, a collagen I-based scaffold, was sparse in both epithelial cell and fibroblast growth. Apparently, the interaction of cells with the various native scaffolds can influence cellular behavior and organization in terms of cell-cell interaction, and lead to different patterns of cellular growth. Furthermore, the epithelial cells seeded on the TF membrane showed an atypical morphology, whereas epithelial cells seeded on BG, BGP, and SIS uniformly covered the respective membranes and displayed typical morphology. This may be linked to the constituents of the respective membranes, as the TF membrane consists only of collagen type I, which is a collagen type expressed in the mature wound, whereas collagen type III, a component of the BG, BGP, and SIS membranes, is expressed predominantly during the granulation phase of the immature wound.³⁴ Collagen III is known for mediating differentiation of cells in wound healing.³⁴ Thus, membranes

containing collagen type III might have a favorable effect on TEOMs formation, as shown in this study.

In natural wound healing, as in the innate process of skin and mucosal recovery and reconstruction, the wound clot containing collagen and fibronectin acts as a matrix, which allows epithelial and fibroblast cells to migrate and close the wounds.²⁰ In tissue engineering, there is a need to replace the wound clot by another matrix or membrane for enabling targeted and orchestrated cellular growth and migration, which mimics the natural process of epithelial and mucosal regeneration, as the successful development of an artificially generated tissue is highly dependent on the scaffold material.³⁵ This was the decisive criterion for the selection of collagen membranes for this study. In the four unique membranes investigated in this study, the tissue engineered mucosa was composed of several layers of epithelial cells and fibroblasts. In addition, a matrix of structural proteins containing collagen and tenascin were formed in all TEOMs. The epithelial cells were able to spread, organize, and form a multi-stratified epithelial layer on the upper side of the various membranes, as shown by cytokeratin 13 immunostaining. This can only be achieved by seeding primary epithelial cells, since polarization is usually not achieved by using epithelial cell lines.³⁶ Collagen IV, a component of the lamina densa of basement membrane,⁷ was detected on the interface between the multi-layered epithelial tissue on all various membranes. Since only mature epithelia synthesize a basement membrane,³⁶ it appears that the epithelial layer of all TEOMs in the experimental models presented here formed a mature tissue-like construct. The formation of a functioning basement membrane is vital for the epithelial layer and for the functionality of the engineered mucosal substitutes, since the basement membrane acts as an anchor for the epithelial layer to the extracellular matrix.^{7,36} Thus, the basement membrane formation in the TEOMs is a sign of a stable epithelial coverage of the distinct scaffolds, an important characteristic with respect to further clinical applications.

For tissue engineering purposes, higher porosity is a prerequisite in the tissue-engineered matrices as it fundamentally influences cellular activity, for example cell proliferation and migration, as well as nutrient and oxygen transport.^{33,37,38} To assess the ability of membranes to support TEOM formation with respect to their 3D architecture, we selected scaffolds with different collagen types, with or without collagen cross-linkage, with different alignment of the collagen fibers, as well as with different membrane density. In this study, no fibroblast migration into the TF membrane was observed after 20 days of fibroblast culture and 16 days of epithelial cell co-culture. This may be due to the low amount of porosity of the TF membrane, as the membrane is compact, displaying a parallel array of the collagen fibers without spaces, making it difficult for the fibroblasts to migrate into the scaffold, as scaffold architecture is well known to direct cell behavior and fate.³³ The architecture of the BG, BGP, and SIS membranes, on the other hand, resembled a meshwork of interwoven collagen proteins, as shown in SEM analyses. This microarchitecture mimics the skin tissue architecture with its meshwork of interwoven proteins resulting in typical mechanical properties, such as elasticity and flexibility.³³ The open porous structure of BG, BGP, and SIS was

expected to facilitate the cellular ingrowth and vascularization after implantation. This effect might be more enhanced in membranes of middle density such as the BG and the BGP membrane, where cord-like structures were clearly visible in SEM analyses, however, less were observed in the SIS membrane. Additionally, the higher level of cross-linking of the BGP membrane might negatively impact the migration of cells,³⁹ as observed in this study. This is in line to other findings, which outlined that the topographic pattern onto which cells were seeded *in vitro* had an impact on cell behavior and differentiation.³³

Fibroblasts play a key role in dermal homeostasis and regeneration of dermal tissue by providing a suitable support framework for neo-angiogenesis and by facilitating epithelialization.^{21,40} Additionally, fibroblasts are responsible for the generation and secretion of extracellular matrix proteins, such as tenascin. Tenascin, a glycoprotein, is an important regulatory factor in wound healing, and is involved in distinct regulatory functions than typical extracellular matrix proteins.⁴¹ Tenascin, which is secreted by specialized contractile wound fibroblasts was detected in the granulation tissue immediately underlying recently migrated epidermis in wounds.⁴¹ In the present study, tenascin was only detected within the scaffolds BG, BGP, and SIS after 20 days of culture and the BG membrane displayed the most abundant tenascin staining. We detected no staining for tenascin in the TF scaffold, since fibroblasts did not migrate into this membrane. However, in contrast to our findings, others have described fibroblast migration into the TF membrane as soon as day 14 of fibroblast culture and day 7 of keratinocytes culture.⁴² Tenascin, a major component of the granulation tissue, has been proposed to play a major role in epidermal wound healing, providing an optimal substrate for the movement of cells across the granulation tissue by coating the collagen fibers, and by promoting the interaction of migrating cells or other extracellular matrix components with collagen.⁴¹ These findings are in line with our results, showing the maximal migration of fibroblasts inside the BG membrane, the membrane exhibiting the largest amount of tenascin formation. Invasion of fibroblasts from the surrounding tissue into a wound requires an activation of the fibroblasts as a result of changes in the extracellular matrix.⁴³ Additionally, delayed migration velocity of fibroblasts might contribute to impaired wound healing.²¹ In our experimental setting, it appears that optimal fibroblast migration and tenascin expression might influence each other during TEOMs formation, a process similar to natural wound healing. In addition, it appears that the unique structure of the BG membrane, derived from non-cross-linked types I and III collagen, may boost the expression and secretion of tenascin by fibroblasts. Additionally, tenascin promote the migration of epithelial cells and thus efficient epithelialization in adult wounds.⁴⁴ The high expression of tenascin formed by the TEOMs on the BG membrane might best mimic the early stages of the physiological wound healing process and might subsequently enhance the cellular migration after implantation in both epithelial cells and fibroblasts. Moreover, the shrinkage of the BG membrane, the scaffold which facilitated the most intense fibroblast invasion, might be a result of fibroblast contraction.^{21,45} This effect may lead to a more rapid wound closure and success of the implant

compared to TEOMs on membranes with lower or no fibroblast migration and respectively, tenascin formation. In this context, the expression of tenascin is an important indicator of appropriate fibroblast function and differentiation in the respective TEOMs.

Thus, we conclude that the BG membrane provided the best microenvironment for cellular growth and development, resulting in the formation of a multi-layered epithelial stratum. In addition, the BG membrane facilitated the attachment, proliferation and migration into the membrane and a cellular organization mimicking *in vivo* tissue. The TEOMs engineered on the BGP and the SIS membranes displayed suboptimal tissue-like structures. Although the BG and BGP membranes contain the same collagen types, the cross-linkage of the collagen in the BGP membrane may increase the matrix rigidity and may impede optimal migration of the fibroblasts into the membrane. Since the culture conditions were identical, we concluded that the BG scaffold architecture, morphology and the ability to retain growth factors and matrix proteins were both crucial and optimal for the development of the 3D cellular network.

All four tested membranes retained a structural stability until formation of TEOMs. No biodegradation was observed up to day 20, or until full formation of the TEOMs *in vitro*. *in vivo* animal studies with rats showed similar effects, since the BG membrane showed only a 60% loss in the amount of collagen at 4 weeks after implantation,⁴⁶ while the SIS membrane was completely resorbed 12 weeks post implantation.⁴⁷ This is important with respect to further clinical applications, as the scaffolds help to maintain the integrity of tissue architecture during wound healing.³³ In contrast, biodegradation was observed after 21 days of cell culture with the TF scaffold.⁴² In addition, the TF membrane was described as very smooth and flexible, with deformations of the surface in places with the greatest cell growth.⁴² In our study, the scaffolds remained stable during the entire *in vitro* culture time of 20 days. Thus, all four scaffolds assessed in this study would meet the criteria for an optimal 3D membrane in a clinical setting, as they would preserve the architecture of the tissue during the regeneration process.³³ In this study, cell viability as well as scaffold structural stability were observed only during *in vitro* cultivation. Further studies are needed for the assessment of the artificial graft regarding *in vivo* biocompatibility and biodegradability, *in vivo* immunogenicity and *in vivo* hemocompatibility, for example by implanting the various tissue engineered grafts subcutaneously in animal models prior to their clinical examination in humans.

Since the genitourinary area undergoes mechanical stress during activities of daily living, ideally, a membrane suitable for engineering TEOMs for tissue replacement in this area should maintain shape and size and should be able to endure mechanical stress during the process of tissue recovery at the implantation site. Additionally, using biodegradable membranes for tissue engineering might facilitate further clinical applications, as the membranes might help to anchor the engineered tissue in the area of interest, for example by direct stitching with the adjacent structures. After implanting engineered tissues into wounds, these engineered grafts could act as the starting point for new tissue regeneration by distributing cells into the wound.³³ Thus, the malleable handling of the BG membrane offer

additional benefits in tissue engineering in areas with physical pressure.³¹ Further, the BG membrane is commercially available and suitable for mass production and thus eligible to provide a point-of-care product for all patients in need.

5 | CONCLUSION

Although the BG membrane showed some physical instability in terms of shrinking during long-term cell culture, it exhibited the best results with respect to TEOMs formation, as it displayed an optimal matrix for cellular growth, proliferation, and stratification. Moreover, secretion of essential extracellular matrix proteins by both epithelial and fibroblast cells was shown. In addition, through its unique porous structure of non-cross-linked types I and III collagen, the BG scaffold provided the optimal mechanical and molecular signaling, promoted fibroblast migration into the membrane and the formation of a 3-dimensional tissue engineered oral mucosal equivalent. Therefore, the TEOMs cultured on the collagen-based BG membrane using the in vitro cell culture system described showed the best potential for further clinical interventions. Nevertheless, further studies are needed to compare the BG membrane and other scaffolds, like acellular dermal matrices (ADM), hydrogels, or combinations.

6 | FUTURE PERSPECTIVES

Developing reproducible and cost-effective 3D engineered mucosa tissues can provide long-term benefits in patients with tissue defects in various body areas like the genitourinary region or the oral and maxillofacial area. Subsequently, this method could act as a precursor technique for the development of tissue engineered skin. This new clinical technology may facilitate treatment in patients with challenging conditions, such as chronic wounds resulting from peripheral vascular disease or diabetes. In addition, tissue engineered skin or mucosa equivalents could be used in patients with wound-healing problems such as preexisting skin conditions arising from irradiated skin, in patients with lichen sclerosus or with recurrent surgeries.

Further studies are needed to promote the development of engineered tissue with autologous cells as well as the establishment of culture conditions following all safety requirements prior to clinical applications. Although tissue engineering is a time consuming and costly process, it may be appropriate for a selected collective of patients. To date, it is technically difficult to engineer custom size-fitting products for larger wounds or areas, but even small surface areas of engineered tissue could lead to an accelerated replenishment of lost tissue, resulting in improved and faster tissue regeneration after the initial injury and leading to a significant improvement in patient care and well-being. Thus, tissue engineering, as an approach for personalized medicine, may increase patient satisfaction, quality of life, and decrease the need for corrective surgery.

ACKNOWLEDGMENTS

We are grateful to Dr. Schäfer and the staff of Geistlich Pharma AG, Wolhusen, Switzerland for providing the BioGide® and BioGidePro® membranes and technical support. We thank Baxter GmbH and Cook Biotech Inc. for providing TissuFoil E®. Thanks also to Tamara Diehl and Anne Sartoris for excellent technical assistance. Open access funding enabled and organized by Projekt DEAL.

REFERENCES

- Jessop ZM, Al-Himdani S, Clement M, Whitaker IS. The challenge for reconstructive surgeons in the twenty-first century: manufacturing tissue-engineered solutions. *Front Surg.* 2015;2 (October):1-5.
- Humby G. A one-stage operation for hypospadias. *Br J Surg.* 1941;29: 84-92.
- Mai C, Bertelmann E. Oral mucosal grafts: old technique in new light. *Ophthalmic Res.* 2013;50(2):91-98.
- Neumann O, Treck H. Free transplantation of oral mucosa in the context of diagnostic and therapeutic laryngofissure. *Arch Klin Exp Ohren Nasen Kehlkopfheilkd.* 1973;205(2):371-376.
- Höckel M, Dornhöfer N. Vulvovaginal reconstruction for neoplastic disease. *Lancet Oncol.* 2008;9(6):559-568.
- Ding JX, Chen LM, Zhang XY, Zhang Y, Hua KQ. Sexual and functional outcomes of vaginoplasty using acellular porcine small intestinal submucosa graft or laparoscopic peritoneal vaginoplasty: a comparative study. *Hum Reprod.* 2015;30(3):581-589.
- Butler CE, Orgill DP. Simultaneous in vivo regeneration of neodermis, epidermis, and basement membrane. *Adv Biochem Eng Biotechnol.* 2005;94:23-41.
- Raya-Rivera AM, Esquiliano D, Fierro-Pastrana R, et al. Tissue-engineered autologous vaginal organs in patients: a pilot cohort study. *Lancet.* 2014;384(9940):329-336.
- Raya-Rivera A, Esquiliano DR, Yoo JJ, Lopez-Bayghen E, Soker S, Atala A. Tissue-engineered autologous urethras for patients who need reconstruction: an observational study. *Lancet.* 2011;377(9772): 1175-1182.
- Atala A. Engineering organs. *Curr Opin Biotechnol.* 2009;20(5):575-592.
- Atala A. Regenerative medicine and tissue engineering in urology. *Urol Clin North Am.* 2009;36(2):199-209.
- Ram-Liebig G, Bednarz J, Stuerzebecher B, et al. Regulatory challenges for autologous tissue engineered products on their way from bench to bedside in Europe. *Adv Drug Deliv Rev.* 2015;82: 181-191.
- Al-Himedani S et al. Tissue-engineered solutions in plastic and reconstructive surgery: principles and practice. *Front Surg.* 2017;4 (February):1-14.
- Özgenel GY, Özcan M. Neovaginal construction with buccal mucosal grafts. *Plast Reconstr Surg.* 2003;111(7):2250-2254.
- Ram-Liebig G, Barbagli G, Heidenreich A, et al. Results of use of tissue-engineered autologous Oral mucosa graft for urethral reconstruction: a multicenter, prospective, observational trial. *EBioMedicine.* 2017;23:185-192.
- Farage MA, Maibach HI. Morphology and physiological changes of genital skin and mucous membranes. *Curr Probl Dermatol.* 2011;40: 9-19.
- Barbagli G, Fossati N, Sansalone S, et al. Prediction of early and late complications after oral mucosal graft harvesting: multivariable analysis from a cohort of 553 consecutive patients. *J Urol.* 2014;191(3): 688-693.
- Fasolis M, Zavattero E, Sedigh O, et al. Oral mucosa harvest for urologic reconstruction: role of maxillofacial surgeon and donor-site morbidity evaluation. *J Craniofac Surg.* 2014;25(2): 604-606.

19. Bhargava S, Patterson JM, Inman RD, MacNeil S, Chapple CR. Tissue-engineered buccal mucosa urethroplasty-clinical outcomes. *Eur Urol*. 2008;53(6):1263-1271.
20. Shaw TJ, Martin P. Wound repair at a glance. *J Cell Sci*. 2009;122(18):3209-3213.
21. Hu MS, Maan ZN, Wu JC, et al. Tissue engineering and regenerative repair in wound healing. *Ann Biomed Eng*. 2014;42(7):1494-1507.
22. Sykes B. The molecular genetics of collagen. *Bioessays*. 1985;3(3):112-117.
23. Heller M, Frerick-Ochs EV, Bauer HK, et al. Tissue engineered pre-vascularized buccal mucosa equivalents utilizing a primary triculture of epithelial cells, endothelial cells and fibroblasts. *Biomaterials*. 2016;77:207-215.
24. Rennekampff HO, Rabbels J, Reinhard V, Becker ST, Schaller HE. Comparing the Vancouver scar scale with the cutometer in the assessment of donor site wounds treated with various dressings in a randomized trial. *J Burn Care Res*. 2006;27(3):345-351.
25. Soiederer EE, Lantz GC, Kazacos EA, Hodde JP, Wiegand RE. Morphologic study of three collagen materials for body wall repair. *J Surg Res*. 2004;118(2):161-175.
26. Ayubi FS, Armstrong PJ, Mattia MS, Parker DM. Abdominal wall hernia repair: a comparison of Permacol[®] and Surgisis[®] grafts in a rat hernia model. *Hernia*. 2008;12(4):373-378.
27. Soergel TM et al. Complications of small intestinal submucosa for corporal body grafting for proximal hypospadias. *J Urol*. 2003;170(4 II):1577-1579.
28. Oda D, Savard CE, Eng L, Sekijima J, Haigh G, Lee SP. Reconstituted human oral and esophageal mucosa in culture. *Vitr Cell Dev Biol Anim*. 1998;34(1):46-52.
29. Goldner J. A modification of the MASSON TRICHROME technique for routine laboratory purposes. *Am J Pathol*. 1938;14(2):237-243.
30. Bhardwaj N, Chouhan D, Mandal BB. *3D Functional Scaffolds for Skin Tissue Engineering*. Amsterdam, Netherlands: Elsevier Ltd; 2018.
31. Willershausen I, Barbeck M, Boehm N, Sader R, Willershausen B, James C. Non-cross-linked collagen type I/III materials enhance cell proliferation: in vitro and in vivo evidence. *J Appl Oral Sci*. 2014;22(1):29-37.
32. Rothamel D, Schwarz F, Suculean A, Herten M, Scherbaum J, Becker W. Biocompatibility of various collagen membranes in cultures of human PDL fibroblasts and human. *Clin Oral Implants Res*. 2004;15(4):443-449.
33. Ho J, Walsh C, Yue D. Current advancements and strategies in tissue engineering for wound healing: a comprehensive review. *Adv Wound Care*. 2017;6(6):191-209.
34. Lambert W, Cohen P, Klein K, Lambert M. Mechanisms in selected concepts. *Clin Dermatol*. 1985;2(3):17-23.
35. Lin C, Bissell MJ. Regulation matrix of cell differentiation by Extracellular. *FASEB J*. 1993;7(9):737-743.
36. Paz AC, Soleas J, Poon JCH, Trieu D, Waddell TK, Mcguigan AP. Challenges and opportunities for tissue-engineering polarized epithelium. *Tissue Eng Pt B*. 2014;20(1):56-72.
37. Zeltinger J, Sherwood JK, Graham DA, Müller R, Griffith LG. Adhesion, proliferation, and matrix deposition. *Tissue Eng*. 2001;7(5):557-572.
38. Sankar D, Chennazhi KP, Nair SV, Jayakumar R. Fabrication of chitin/poly(3-hydroxybutyrate-co-3-hydroxyvalerate) hydrogel scaffold. *Carbohydr Polym*. 2012;90(1):725-729.
39. Thoma DS, Villar CC, Cochran DL, Hämmerle CHF, Jung RE. Tissue integration of collagen-based matrices: an experimental study in mice. *Clin Oral Implants Res*. 2012;23(12):1333-1339.
40. Gosain A, DiPietro LA. Aging and wound healing. *World J Surg*. 2004;28(3):321-326.
41. Mackie EJ, Halfter W, Liverani D. Induction of tenascin in healing wounds. *J Cell Biol*. 1988;107(6):2757-2767.
42. Kriegebaum U, Mildenberger M, Mueller-richter UDA, Klammert U, Kuebler AC, Reuther T. Tissue engineering of human oral mucosa on different scaffolds: in vitro experiments as a basis for clinical applications. *Oral Maxillofac Surg*. 2012;114(5):S190-S198.
43. Hinz B. The role of myofibroblasts in wound healing. *Curr Res Transl Med*. 2016;64(4):171-177.
44. Midwood KS, Williams LV, Schwarzbauer JE. Tissue repair and the dynamics of the extracellular matrix. *Int J Biochem Cell Biol*. 2004;36(6):1031-1037.
45. Li B, Wang JHC. Fibroblasts and myofibroblasts in wound healing: force generation and measurement. *J Tissue Viability*. 2011;20(4):108-120.
46. Kozlovsky A, Aboodi G, Moses O, et al. Bio-degradation of a resorbable collagen membrane (bio-Gide[®]) applied in a double-layer technique in rats. *Clin Oral Implants Res*. 2009;20(10):1116-1123.
47. Sandusky GE, Badylak SF, Morff RJ, Johnson WD, Lantz G. Histologic findings after in vivo placement of small intestine submucosal vascular grafts and saphenous vein grafts in the carotid artery in dogs. *Am J Pathol*. 1992;140(2):317-324.

How to cite this article: Schwab R, Heller M, Pfeifer C, et al. Full-thickness tissue engineered oral mucosa for genitourinary reconstruction: A comparison of different collagen-based biodegradable membranes. *J Biomed Mater Res*. 2021;109:572-583. <https://doi.org/10.1002/jbm.b.34724>